27th International Congress on Sound and Vibration
The annual congress of the International Institute of Acoustics and Vibration (IIAV)
11-16 July, 2021
ICSV27

Annual Congress of the International Institute of Acoustics and Vibration (IIAV)

NONLINEARITY OF BALANCED MEMS LOUDSPEAKERS: OPTICAL EXPERIMENTS AND NUMERICAL MODELING USING TIME-HARMONIC SIGNALS

Anton Melnikov, Stolz Michael, Franziska Wall, Bert Kaiser, Andreas Mrosk, David Schuffenhauer, Jorge Monsalve, Langa Sergiu
Fraunhofer Institute for Photonic Microsystems IPMS, Dresden, Germany
e-mail: anton.melnikov@ipms.fraunhofer.de
Hermann A. G. Schenk, Lutz Ehrig, Holger Conrad
Arioso Systems GmbH, Dresden, Germany
email: hermann.schenk@arioso-systems.com
Maik Ahnert
Fraunhofer Institute for Machine Tools and Forming Technology IWU, Dresden, Germany
Harald Schenk
Fraunhofer Institute for Photonic Microsystems IPMS, Dresden, Germany
Brandenburg Technical University Cottbus-Senftenberg BTU, Micro and Nano Systems, Cottbus, Germany

A recently introduced novel actuator class, called the nano electrostatic drive (NED), uses the electrostatic actuation to generate large deflections of elastic structures. The NED principle was recently successfully applied to create an all silicon loudspeaker based on micro-electro-mechanical systems (MEMS) technology. Such MEMS audio transducers cover the full frequency range required for high fidelity audio applications. High fidelity audio reproduction also demands minimizing harmonic distortions substantially below 1 %. A major advance in this direction is combining the NED principle with a push-pull driving scheme in a balanced design (BNED), eliminating even harmonics. The practical implementation of a BNED design is however demanding. The nature of the Coulomb force, the impact of stress stiffening and the large deformations required for generating high sound pressures, to name a few aspects, potentially contribute to the harmonic distortion and therefore need advanced experimental methods and simulation models to allow for an apt design. In this paper, we report first results of an experimental technique, combining an optical microscope with a high-speed camera, capable of analyzing the local details of the actuator movement at frame rates of 50,000 frames per second. Dynamic features, such as the excitation of harmonics and intermodulations become clearly visible. These experimental results are then used to scrutinize and refine our multi physics FEM simulations.
Keywords: electroacoustics, MEMS, loudspeakers, balanced, nonlinear

1. Introduction

MEMS based microspeakers (μSpeakers) are a new and rapidly developing field in electroacoustics. The recently developed nanoscopic electrostatic drive (NED) technology [1] offers a high potential for

electrostatic transducers for audio and ultrasound applications. Kaiser *et al.* demonstrated the experimental realization of an all-silicon micro-speaker based on the NED approach [2]. Such loudspeakers can be manufactured by a processes entirely compatible with complementary metal-oxide-semiconductor (CMOS) technology. This paves the way for high fidelity μSpeakers for in-ear audio reproduction, far superior in size and power efficiency, based on a silicon technology with the potential to claim cost-leadership in mass markets. A second key step towards practical applications was demonstrated by combining the NED technology with the push-pull drive principle [3]. To build a push-pull NED actuator, a special kind of cantilever structure is required [3] and this places new challenges for modelling. Spitz *et al.* [4] experimentally extracted parameters to fit a nonlinear single-degree-of-freedom differential equation in order to model the large signal response of an asymmetric NED (ANED) based μSpeaker. This observation gave rise to the development of efficient large signal reduced order models for microbeams [5, 6], capable of reproducing the overall actuator dynamics of a well designed actuator with surprising accuracy. Monsalve *et al.* [7] used a finite element method (FEM) as well as the mentioned lumped parameter models to extract the nonlinear electro-mechanical parameters for the successful equivalent circuit modelling of ANED and BNED devices. However relating a subtle detail, such as a comparatively minute harmonic distortion, to the details of an actuator design under development, goes far beyond the reach of modelling methods, which reduce the complexity of the actuator dynamics to a single degree of freedom. Substantially more powerful ab-initio modelling methods, firmly based on clear experimental evidence, are required to this end. To tackle this challenge, we propose the technique of high-speed recording of micrographs in combination with digital object tracking. This allows to resolve the transient movement of microstructures in full detail at different geometric locations. The experimental results can be compared to transient multiphysics FEM simulations. This provides the required deep insight into the nonlinear dynamics and thus allows for refined time dependent FEM models.

2. Method

A high-speed Photron Fastcam SA1.1 camera was mounted on top of a Leica DM8000 microscope, see Fig. 1(a). The details of the BNED dynamics were tracked using a 500x magnification and a frame rate of 50 kfps. A typical micrograph with a frame resolution of 192×160 pixels is shown in Fig. 1. A total of 11036 frames were recorded while the actuator was excited with a signal frequency of 1 kHz. At least 220 periods of steady-state oscillation were captured during 221 ms of measurement time. In a second part of the experiment, a total of 5001 frames were recorded at 9 kHz excitation frequency. This allowed to capture 900 periods of steady state oscillations within a time span of 100 ms.

The sinusoidal signal voltage with an amplitude of 10 V was supplied to the middle electrode of the BNED by a Tektronix AFG3102C frequency generator. In addition to the AC signal, a DC voltage of $\pm 11\,\mathrm{V}$ was applied to the outer BNED electrodes. The DC voltage supply and the control of the leakage current between the electrodes was realized using a Keysight B2912A precision source measure unit. All bond pads of the sample were contacted manually directly on the wafer by means of tungsten needles using Imina Tec MiBots.

For evaluation, the deflection of the BNED was tracked by the Lucas-Kanade method as provided in the python library OpenCV. In particular, a single marker at the center beam was set (see red marker in Fig. 1(b)) and its trajectory in the image plane was extracted. The deflection in y-axis was used to calculate the deflection spectra presented in Section 3.

The FEM modelling was based on COMSOL Multiphysics 5.6. The structural domain and the electrostatic domain were discretized with 2D second order serendipity elements. The FEM mesh is shown in Fig. 2, where different colors indicate domains and materials. For more details on the structure itself and its function description see Ref. [3]. The structural domain was solved including nonlinear strains and

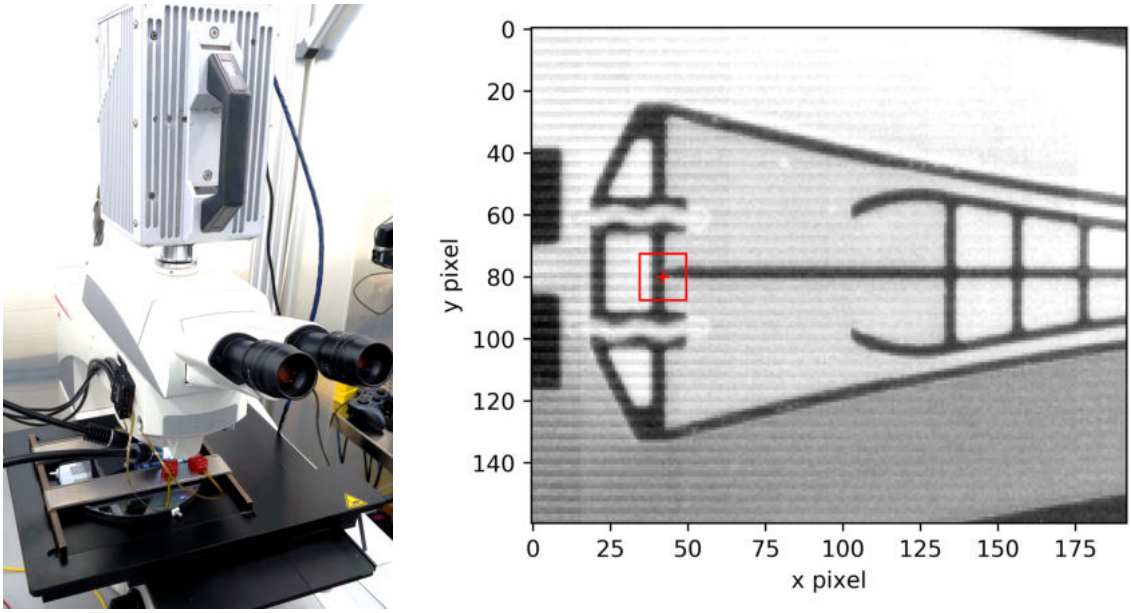

(a) (b)

Figure 1: (a) The measurement setup: The Photron Fastcam SA1.1 high-speed camera on top of the Leica DM8000 microscope. (b) A micrograph of the free end of the BNED structure. The red marker shows the pattern tracking location used for the extraction of the movement.

large deformations. The silicon (Si) was modelled with the anisotropic parameters provided by Hopcroft *et al.* [8]. The electrostatic domain was solved considering the impact of large structural deflections. This was necessary model the non-linearity of the electrostatic forces in full detail. The time discretization was 60 steps per excitation period.

3. Results

3.1 Selection of the operating point and excitation frequencies

The eigenfrequency of an electrostatically actuated MEMS cantilever varies depending on the applied voltage [9, 10, 11]. The voltage dependent frequency shift for the first BNED bending mode, as computed by means of a FEM modal analysis that includes all nonlinear effects, is shown in Fig. 3. The frequency decreases with increasing voltage until it runs into the pull-instability, where it reaches zero. This yields a pull-in voltage of $U_{\mathrm{DC}} = 35.3\,\mathrm{V}$. The operating point used in our experiment, was selected to be $U_{\mathrm{DC}} = 11\,\mathrm{V}$ and $f_0 = 4072.9\,\mathrm{Hz}$. The operating point is indicated by the green lines in Fig. 3. The excitation frequencies of 1 kHz and 9 kHz were selected for our experiment to lie below and above the eigenfrequency of the first cantilever bending mode.

3.2 Excitation below the eigenfrequency

Figure 4(a) shows the measured deflection spectrum (red solid line) of a BNED test structure, tracked at the location indicated by the red marker in Fig. 1(b)). As expected, the excitation frequency of 1 kHz (fundamental) is observed with the largest magnitude of $\hat{u}_y \approx 2\,\mu\mathrm{m}$. The third and fifth harmonic dominate the harmonic distortion. The second order harmonic is somewhat smaller. This demonstrates the effect of the push-pull approach, which aims to reduce the contribution of the even harmonics [3]. In

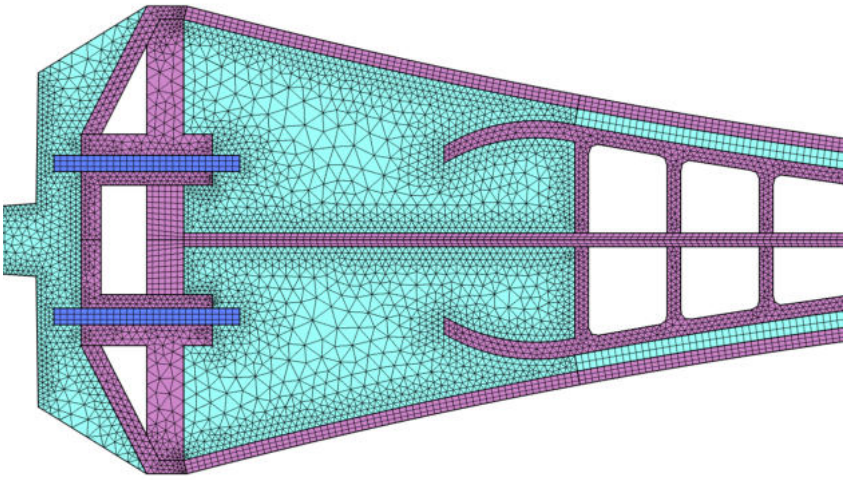

Figure 2: The free end of a sample BNED structure showing the FEM discretization. The pink and the blue region corresponds to the structural domain indicating Si and dielectric, accordingly. The cyan regions represent the electrostatic domain filled with air.

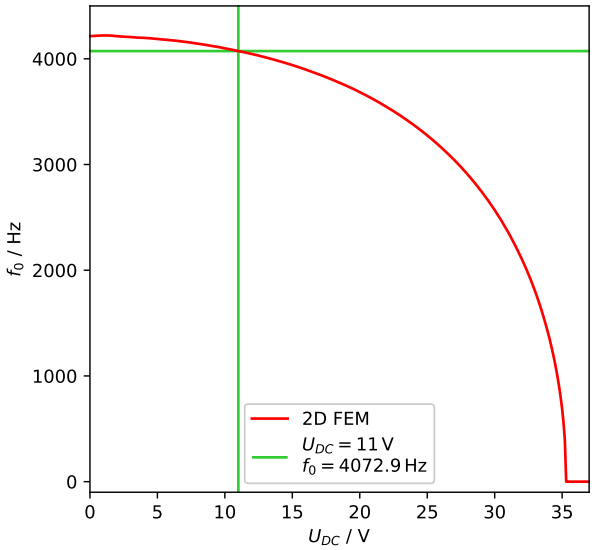

Figure 3: The shift of the lowest BNED eigenfrequency depending on the applied DC voltage. The pull-in instability can be identified at the voltage, where the eigenfrequency drops to zero.

case of an ANED, the second order harmonic is by far the most prominent feature, with an amplitude depending on the DC bias [11].

The spectra from the FEM simulation are shown in Fig. 4(a) as black and blue squares. The black squares represent the results when the electrostatic potential around the tip of the BNED actuator is not considered. In this FEM model, the deflection is only generated by the electrostatic field in the electrode gap within the NED actuator. When compared to the FEM simulation, the fundamental oscillation and the third harmonics qualitatively match the experimental results. However, the contributions of second and fifth harmonics are underestimated. The electric field surrounding the tip of the BNED was therefore included into a refined FEM model (see blue squares in Fig. 4(a)). This resulted in an improved match with our experiment, regarding the even harmonics and the fifth harmonic. Nevertheless, the fifth harmonics is still underestimated.

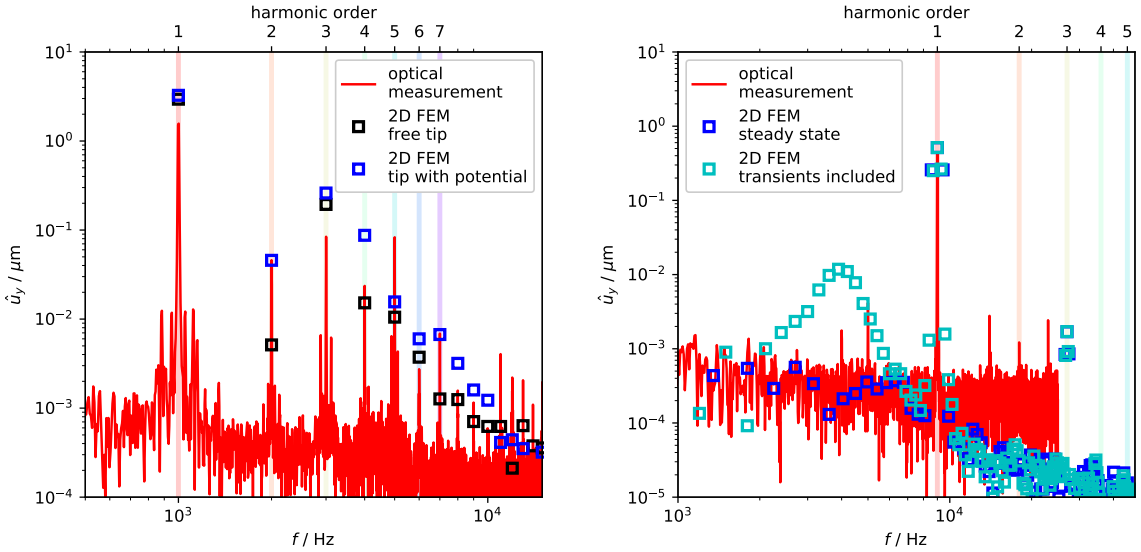

Figure 4: Experimentally and numerically determined deflection spectra on the tip of the BNED test structure at location corresponding to the red marker in Fig. 1(b). (a) Excitation below the eigenfrequency with 1 kHz. (b) Excitation above the eigenfrequency with 9 kHz.

3.3 Excitation above the eigenfrequency

Figure 4(b) shows the experimentally determined deflection spectrum using a 9 kHz excitation as a red solid line. The second harmonic is present in the spectrum. However its contribution is much lower compared to the excitation at 1 kHz. Since the frame rate of the high-speed camera was 50 kHz, the experimental spectrum is limited to below 25 kHz, according to the Nyquist–Shannon sampling theorem. For that reason, the contribution of the third harmonic at 27 kHz was not captured in our experiment. Furthermore, the experimental spectrum contains additional harmonics, that are not integer multiples of the excitation frequency. Clarifying their origin needs further attention.

The FEM results for the excitation at 9 kHz are shown as blue and cyan squares in Fig. 4(b).The blue squares represent the steady-state situation, while the cyan squares exhibit the influence of transients. In both simulations the electrical field distribution at the tip of the BNED was included. There is no contribution of the second harmonic predicted by the FEM simulation, which is expected for an ideal implementation of a push-pull actuation. The contribution of the third harmonic is below 1 % compared

to the excitation frequency. When transient effects are considered (cyan squares in FIg. 4(b)), a broad Lorentian-like shape with a peak around 4 kHz arises. This is an oscillation related to the first BNED bending mode, which does not contribute to steady-state oscillation (blue squares in Fig. 4(b)).

4. Discussion

The analyzed BNED test structure combines the NED principle with a push-pull driving scheme. The design is targeting to reduce the total harmonic distortion by suppressing the even harmonics. This effect was confirmed experimentally using a high-speed camera. Comparing our experimental findings with FEM simulations which were assuming an ideal actuator geometry, we recognized that some experimental features are not yet captured by our numerical models. For example, the fifth harmonics exhibited by the dynamics of our test structure at 1 kHz was not accurately predicted. Including the electrostatic environment at the tip of our test structure, improved the match between experiment and simulation (see Fig. 4(a)). In fact, Fig. 4(a) demonstrates the significant impact of additional geometric features, such as the tip potential distribution, on the spectral fingerprint.

At the excitation frequency of 9 kHz we observed higher harmonics, that are not integer multiples of the excitation frequency, e.g. at 14 kHz. The origin of this feature remains to be explained. The hypotheses that these peaks are due to a transient intermodulation product of the eigenfrequency of the first beam bending mode does not substantiate, see Fig. 5. This is because i) a detailed transient FEM analysis, see Fig. 4(b), shows a broad shoulder in the spectrum rather than a sharp peak and ii) because a potential impact of a transient beam motion is not compatible with our experimental procedure, which allowed the beam to oscillate several seconds before the high-speed recorder was launched.

The most probable root causes for the remaining discrepancies between experiment and theory are manufacturing tolerances and 3D effects, indicating the need to refine our FEM models. In summary the work presented here demonstrates that capturing a MEMS actuator motion with a high-speed camera provides in combination with advanced FEM models an excellent framework to assess the quality of manufactured microstructures and allows furthermore to validate and refine dynamic FEM simulations.

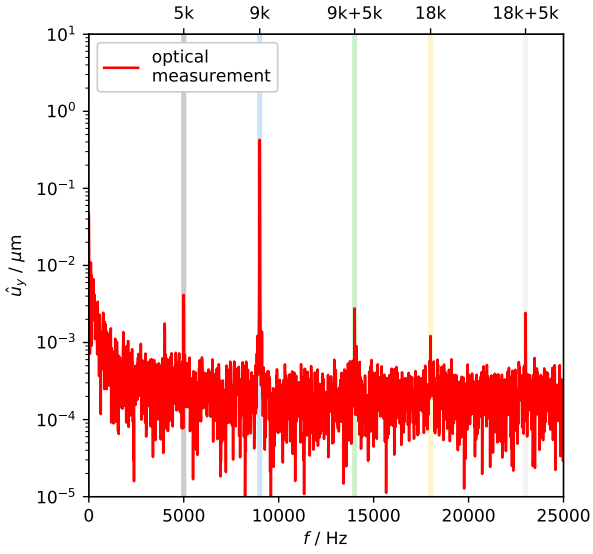

Figure 5: Experimentally determined deflection spectra on the tip of the BNED test structure illustrating a hypothesis of the intermodulation.

5. Conclusion

A MEMS BNED actuator was studied using a high-speed camera and advanced multiphysics FEM simulations. We demonstrated how the nonlinear behaviour of microstructures can be experimentally analyzed by recording the beam dynamics at high frame rates in combination with image analysis using object tracking methods. Furthermore, we experimentally confirmed a significant reduction of the even harmonics, in particular the second harmonic, when the NED design is combined with the principle of push-pull actuation. At the same time, we demonstrated a multiphysics FEM model, which was able to explain most ob the experimentally observed features, while still leaving room for further improvements.

REFERENCES

1. Conrad, H., Schenk, H., Kaiser, B., Langa, S., Gaudet, M., Schimmanz, K., Stolz, M. and Lenz, M. A small-gap electrostatic micro-actuator for large deflections, *Nature Communications*, **6** (1), 1–7.

2. Kaiser, B., Langa, S., Ehrig, L., Stolz, M., Schenk, H., Conrad, H., Schenk, H., Schimmanz, K. and Schuffenhauer, D. Concept and proof for an all-silicon MEMS micro speaker utilizing air chambers, *Microsystems & Nanoengineering*, **5** (1), 1–11, (2019).

3. Kaiser, B., et al. Electrostatic push-pull bending actuator for low distortion acoustic transducers, (2021).

4. Spitz, B., et al. Audio-Transducer for In-Ear-Applications based on CMOS compatible electrostatic actuators, *MikroSystemTechnik Kongress Proceedings*, (2019).

5. Melnikov, A., Schenk, H. A. G., Monsalve, J. M., Wall, F., Stolz, M., Mrosk, A., Langa, S. and Kaiser, B. Coulomb-actuated microbeams revisited: Experimental and numerical modal decomposition of the saddle-node bifurcation, (2021).

6. Schenk, H. A. G., Melnikov, A., Wall, F., Gaudet, M., Stolz, M., Schuffenhauer, D. and Kaiser, B. Coulomb actuated microbeams revisited: Highly efficient lumped parameter models - a chebyshev-edgeworth approach, (2021).

7. Monsalve, J. M., Melnikov, A., Kaiser, B., Schuffenhauer, D., Stolz, M., Ehrig, L., Schenk, H. A., Conrad, H. and Schenk, H. Large-signal equivalent-circuit model of asymmetric electrostatic transducers, (2021).

8. Hopcroft, M. A., Nix, W. D. and Kenny, T. W. What is the Young's Modulus of Silicon?, *Journal of Microelectromechanical Systems*, **19** (2), 229–238, (2010).

9. M. I. Younis and A. H. Nayfeh. A Study of the Nonlinear Response of a Resonant Microbeam to an Electric Actuation, *Nonlinear Dynamics*, **31** (1), 91–117, (2003).

10. Younis, M. I., *MEMS Linear and Nonlinear Statics and Dynamics*, vol. 20 of *Microsystems*, Springer Science+Business Media LLC, Boston, MA (2011).

11. Melnikov, A., Schenk, H. A. G., Wall, F., Spitz, B., Ehrig, L., Langa, S., Stolz, M., Kaiser, B., Conrad, H. and Schenk, H. Minimization of nonlinearities in nano electrostatic drive actuators using validated coupled-field simulation, p. 112930D, International Society for Optics and Photonics, (2020).